Dry mechanochemical synthesis of highly luminescent, blue and green hybrid perovskite solids

Laura Martínez-Sarti, Francisco Palazon, Michele Sessolo and Henk J. Bolink*

L. Martínez-Sarti, Dr. F. Palazon, Dr. M. Sessolo, Prof. H. J. Bolink
Instituto de Ciencia Molecular, Universidad de Valencia
C/ Catedrático José Beltrán, 2, 46980 Paterna, Spain
E-mail: michele.sessolo@uv.es

Keywords: perovskite, mechanochemical synthesis, photoluminescence, blue, passivation

Abstract

A simple method to obtain bright photoluminescent wide bandgap mixed-halide 3D perovskites is reported. The materials are prepared by dry mechanochemical synthesis (ball-milling) starting from neat binary precursors, and show enhanced photoluminescence upon the addition of an adamantane derivative in the precursors mixture. The structural characterization suggest that the additive does not participate in the crystal structure of the perovskite, which remains unvaried even with high loading of amantadine hydrochloride. By simple stoichiometric control of the halide precursors, the photoluminescence can be finely tuned from the UV to the green part of the visible spectrum. Photoluminescence quantum yields as high as 29% and 5% have been obtained for green- and blue-emitting perovskite solids, determined at very low excitation densities.

Metal halide perovskites are being studied for several applications, such as light-emitting diodes, solar cells, photodetectors, lasers, water splitting or memristors.[1][2][3][4][5][6][7][8] This wide application spectrum is enabled by their remarkable optical and electronic properties, among which are their high absorption coefficient, defect tolerance, ambipolar and large charge diffusion length, and high rate of radiative recombination.[9][10][11][12][13] Some of the key factors to obtain high quality perovskites are the purity of the perovskite precursors, the choice of the most appropriate synthetic method, and the control over the environmental processing conditions.[14,15] Solution-based techniques are widely adopted to prepare perovskite compounds. Small amounts of additives (if the solubility in the common solvent is sufficient) or different chemical precursors are often used.[16–18] Also, high boiling point (toxic) solvents, and multiple processing steps,[19,20] are needed to ensure the formation of highly crystalline materials. Solvent-free "dry" mechanochemical synthesis is an alternative technique to prepare perovskites with virtually any composition. It is a simple method which can lead to higher purity due to the absence of processing additives and solvents.[21–23][24–28] Mechanochemical synthesis can be used to synthesize multi-component compounds simply by mixing the chemical precursors in the appropriate stoichiometry. Importantly, there is no limitation to the compositional freedom from the solubility of the precursor salts. Moreover, mechanochemically-synthesized perovskites have demonstrated enhanced stability, which has been attributed to a high purity and a superior crystallinity of the materials in the powder form, resulting in stronger ionic interactions within the crystal lattices.[29,30] Additionally, it has been shown for some perovskites that they can be processed into thin film using single-source vacuum deposition of pre-synthesized compounds,[31][32] allowing the formation of high-quality perovskite thin films.[33][34] Other techniques such as aerosol deposition method are also being developed.[35]

Mechanochemical synthesis is therefore ideally suited to explore wide bandgap, mixed halide perovskites, where the bandgap can be systematically increased by substitution of iodide with

bromide and chloride.[36][37–39] Wide bandgap perovskites are particularly interesting for the fabrication of tandem solar cells and for the development of blue light-emitting diodes.[3,40,41] However, producing stable and luminescent wide bandgap perovskites remains challenging, as pure or chloride-rich compounds typically show low photoluminescence quantum yield (PLQY).[38,39,42] Furthermore, mixed halide materials suffer from photoinduced halide segregation,[43,44] which further complicates the preparation of efficient and stable blue-emitting lead halide perovskites. The addition of passivating agents can be beneficial for the enhancement of the PLQY,[45–47] as they can decrease the density of trap states at the grain boundaries and on the surface.

In this work, we describe the mechanochemical synthesis of stable mixed-cation/mixed-halide perovskites with emission spanning the blue to green region of the visible spectrum. We demonstrate that strong enhancements in the PLQY are obtained by the addition of amantadine hydrochloride to the precursor mix prior to the ball-milling. The effect of this additive is studied as a function of its concentration, and only minor structural changes are observed in the resulting perovskites. Mixed-cation/mixed-halide perovskites, with the general formula $MA_{1-y}Cs_yPb(Br_nCl_{1-n})_3$ (where MA stands for methylammonium) can be easily modified to fine-tune their optical properties. $MA_{0.8}Cs_{0.2}Pb(Br_{0.6}Cl_{0.4})_3$ was chosen as the starting material because this particular halide ratio has a bandgap energy corresponding to the blue region of the electromagnetic spectrum, and the addition of small amounts of Cs brings ambient and structural stability to the perovskite.[48] The precursors, CsBr, CsCl, MABr, MACl, $PbBr_2$ and $PbCl_2$ were mixed accordingly to the targeted compound's stoichiometry $MA_{0.8}Cs_{0.2}Pb(Br_{0.6}Cl_{0.4})_3$ inside a nitrogen-filled glovebox and introduced in a 10 mL zirconia ball-mill jar together with zirconia beads. Afterwards, ball-milling was performed at a frequency of 30 Hz for 2 hours (see experimental section for details).

The as-prepared materials, obtained in powder form, were analysed using x-ray diffraction to determine their structure and by optical spectroscopy to determine their absorption and

luminescence spectral features. The X-ray diffraction (XRD) analysis (**Figure 1**a, black line, 0%) shows intense reflections centred between the reference peaks of pure-bromide $MAPbBr_3$ (ICSD 158306) and pure-chloride $MAPbCl_3$ (ICSD 241415) perovskites, demonstrating the presence of a single mixed-halide phase (the presence of 20% Cs^+ also shifts the XRD signal with respect to pure-methylammonium reference patterns, although this shift is less significant). Hence, the structural analysis confirms the formation of the desired compound. Its optical absorption was measured by placing the powder in a quartz Petri dish into an integrating sphere (Figure 1b, black line, 0%). The material presents a steep absorption onset at about 500 nm (corresponding to a bandgap energy, E_g, of approximately 2.5 eV), in agreement with previous reports on similar compositions.[49] We were not able to detect any photoluminescence, even when the sample was directly irradiated by a UV (375 nm, 100 mW) continuous wave (CW) laser. This is not surprising, as non-passivated, bulk, wide bandgap semiconductors are prone to suffer from non-radiative charge recombination due to a large density of trap states at the surface or grain boundaries.[50] With the aim of reducing the trap states responsible for non-radiative charge recombination, we added amantadine hydrochloride (or 1-adamantanamine hydrochloride, herein after referred to as AmCl) to the precursors of the mechanochemical synthesis. We chose this particular compound in view of its steric hindrance, which would not favour the formation of layered perovskite compounds. Similar molecules have been employed previously in the synthesis of perovskites,[51,52] either to passivate the material[53][54] or for device encapsulation.[48] Here the additive AmCl was introduced in the synthesis in excess with respect to the perovskite precursors, varying its molar ratio (with respect to lead) from 0 to 90 mol%. Importantly, for this specific set of precursors, their solubility in common polar organic solvents is not sufficient to explore the range of composition allowed by mechanochemical synthesis.

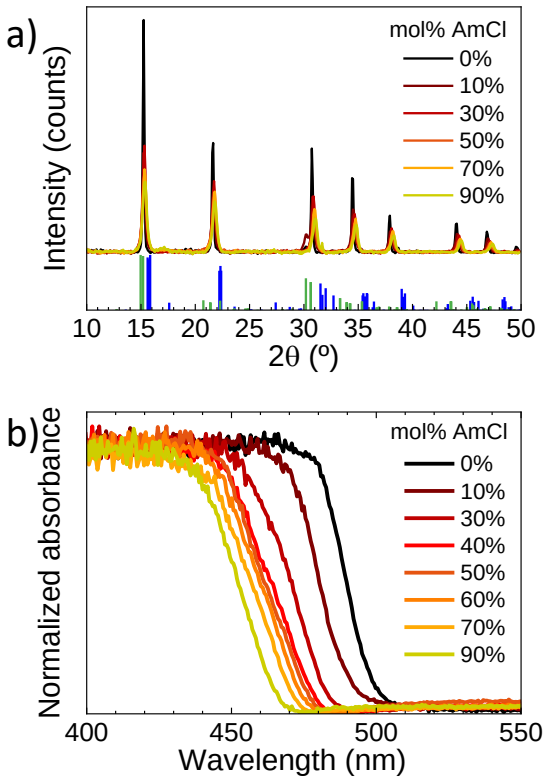

Figure 1. a) XRD patterns for $MA_{0.8}Cs_{0.2}Pb(Br_{0.6}Cl_{0.4})_3$ powders with increasing molar concentration of AmCl and reference bulk pattern (bottom) for $MAPbCl_3$ (blue, ICSD collection code 241415) and $MAPbBr_3$ (green, ICSD collection code 158306). b) Absorption spectra for the same series of materials.

It is important to note that, the use of the chloride salt AmCl inevitably results in the incorporation of excess chloride into the material. Indeed, the optical absorption onset shifts to shorter wavelengths (i.e. the bandgap is widened) with increasing amount of AmCl (Figure 1b). At the same time, the XRD analysis shows a very similar pattern for the whole series, independently on the concentration of AmCl (Figure 1a). This means that the addition of AmCl does not lead to the formation or segregation of different phases but maintains a homogeneous single (mixed-halide) perovskite phase. This can be a consequence of the higher reactivity of MAX and CsX towards PbX_2, which are stoichiometrically added in order to obtain the perovskite $MA_{0.8}Cs_{0.2}Pb(Br_{0.6}Cl_{0.4})_3$, precluding the formation of any compound between

AmCl and the other reagents. Beside a small shift to higher angle, caused by the increased incorporation of the smaller chloride anion, when more AmCl is used the intensity of the peaks decreases and their full width at half maximum increases (see also Figure S1 for details.). These observations might indicate the formation of smaller crystal domains or in general a reduced crystallinity of the materials. From electron microscopy analysis (Figure S8), however, we could not identify any clear trend of the material crystallinity as a function of the additive content, neither a correlation with the PLQY. Most likely, AmCl is still present in the synthesis product but it is amorphous and/or distributed at the grain boundaries. While the XRD analysis confirms that AmCl is not incorporated within the perovskite structure, additional experiments show that the additive can indeed react with Pb(II). When only AmCl and $PbCl_2$ are ball milled in a 2:1 molar ratio, the XRD of the resulting powders does not present any of the $PbCl_2$ characteristic diffraction peaks, while new signals centred at 2θ = 10.3, 15.4, 17.1° appear (Figure S2). No reference XRD pattern was found for this new material, but most likely it is an octahedral polymeric structure similar to others reported in the literature for lead halide coordination compounds.[55]

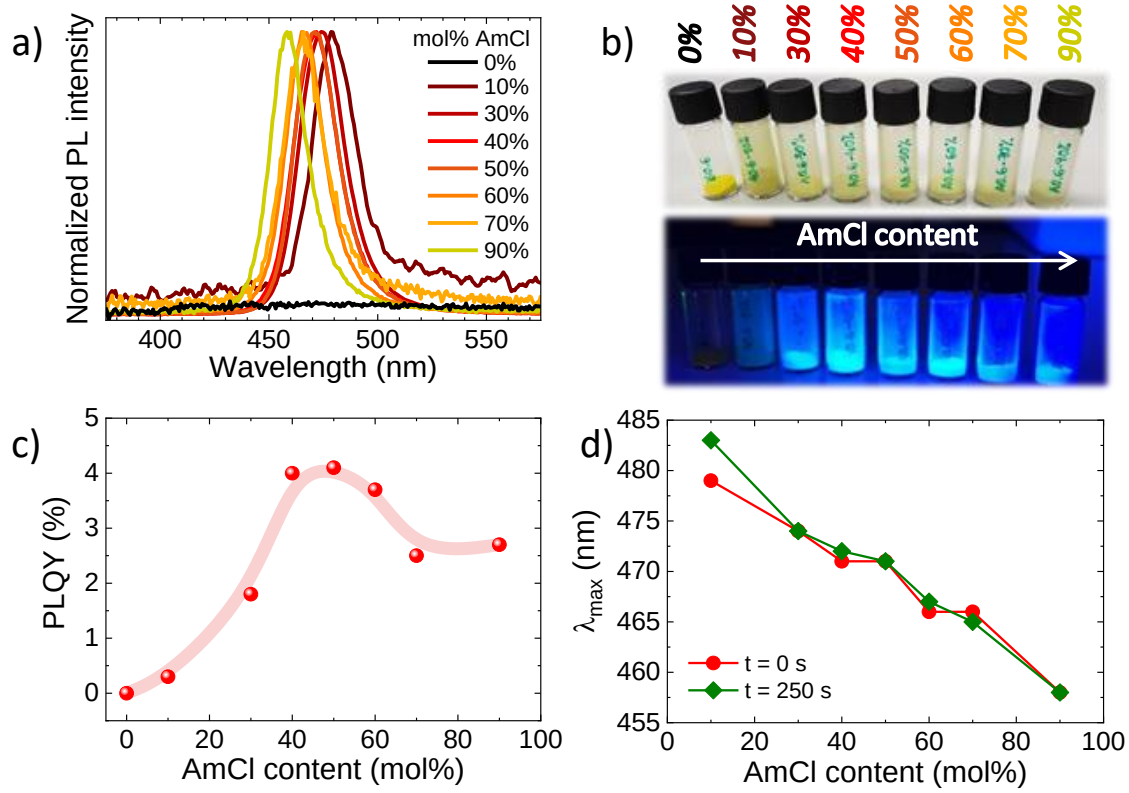

Figure 2. (a) Photoluminescence spectra (λ_{exc} = 375 nm) displayed by the $MA_{0.8}Cs_{0.2}Pb(Br_{0.6}Cl_{0.4})_3$ powders with varying addition of AmCl passivating agent going from 0 mol% to 90 mol%. (b) Photographs taken under ambient light (above) and UV light (λ = 365 nm) (below). (c) PLQY values (the line is a guide to the eye) and (d) first and last measurements of the photo-stability test of the maximum peaks wavelength plotted as a function of the added mol% of AmCl.

The fact that AmCl does not participate into the crystal structure of the $MA_{0.8}Cs_{0.2}Pb(Br_{0.6}Cl_{0.4})_3$ while it can form complexes with Pb(II), suggests that AmCl can indeed interact with the perovskite to passivate surface traps. The origin of the enhanced optical properties in the presence of AmCl is not completely clear, but we exclude an effect of the chloride anion as its incorporation via other ammonium cations does not lead to any appreciable increase in photoluminescence (Figure S7). As a matter of fact, we were able to detect photoluminescence from the perovskite, when synthesized in the presence of AmCl. As observed from the optical

absorption, the increasing amount of chloride causes a blue-shift in the PL emission (**Figure 2**a), with the PL maxima at most shifting from 478 nm to 458 nm when the AmCl concentration is increased from 10 mol% to 90 mol%, respectively (an increase in the bandgap of about 0.1 eV). Thanks to the presence of AmCl, the powders show luminescence already when illuminated with a low-intensity UV lamp (Figure 2b). The AmCl additive is thus capable to passivate the $MA_{0.8}Cs_{0.2}Pb(Br_{0.6}Cl_{0.4})_3$ bulk material, as the PLQY increased from 0 to 4% for AmCl concentration of 40-50 mol%. It is worth to note that the PLQY was measured in an integrating sphere using a Xe lamp coupled to a monochromator as the excitation source, resulting in a very low photogenerated carrier concentration. This implies that the density of trap states is substantially reduced in the presence of AmCl. For AmCl concentrations >50 mol%, the PLQY was found to slightly decrease (Figure 3a). The PLQY reduction is not yet fully rationalized, but can be ascribed to a diminished crystallinity (as evidenced by the XRD analysis) and to the wider bandgap of the material, i.e. not-quenching shallow traps become deep traps favouring non-radiative recombination. $MA_{0.8}Cs_{0.2}Pb(Br_{0.6}Cl_{0.4})_3$ powders containing 50 mol% AmCl were further analysed by X-ray photoelectron spectroscopy (XPS) in order to investigate the elemental composition (Figure S9). The elemental analysis was found to be in good agreement with the compound stoichiometry (Cs = 0.3, Pb = 1, Br = 1.8, Cl = 1.5), taking into account the amount of AmCl used.

As mentioned before, mixed halide perovskites can undergo halide segregation under illumination.[56][44,45] In this regard, the material photostability was studied by monitoring the PL spectra as a function of time, under continuous irradiation. The position of the PL maxima as a function of the AmCl concentration at time 0 and after 250 s is reported in Figure 2d (see Figure S3 in the Supporting Information for further details). We observed only a small shift in the maximum PL intensity only at low AmCl concentration (10 mol%), while for the rest of the samples no change in the optical properties (sign of halide segregation) was detected.

We further studied the effect of the composition on the optical properties of the perovskite by exchanging the A-site cation and the X-site halide anion. The amount of Cs^+ was varied in the mechanochemical synthesis of $MA_{1-y}Cs_yPb(Br_{0.6}Cl_{0.4})_3$ from y = 0 (pure MA^+) to 0.2, 0.4 and 1 (pure Cs^+), maintaining a 50 mol% AmCl concentration. A small deviation in the bandgap of the material was observed upon exchanging MA^+ with Cs^+, as evidenced by the optical absorption spectra (**Figure 3**a) with the hybrid perovskite having larger bandgap as compared to the inorganic one. Also the PL spectra showed a small shift from 467 nm to 472 nm when y was varied from 0 to 1. The structural characterization (Figure 3c) showed again a high degree of conversion and crystallinity for the series of compounds, with an expected shift to larger angles upon substitution with the smaller caesium cation. The different intensity of the main diffraction peaks between the hybrid and fully inorganic perovskites (y = 1) agrees with the slightly different orientation of the unit cell.[57] The concentration of Cs in this perovskite series was confirmed by XPS (Figure S10, Table S4). Interestingly, we found the PLQY to scale inversely with the amount of Cs^+ used in the synthesis of the perovskite $MA_{1-y}Cs_yPb(Br_{0.6}Cl_{0.4})_3$, with the pure MA^+ materials exhibiting blue emission with 7% PLQY. As the caesium content increases, the PLQY progressively decreases to approximately 1% for the pure inorganic compound (y = 1). This behaviour has been previously attributed to the large dipole moment (2.3 D) and rotational freedom of the MA^+ cation, which would respond to the formation of trapped charges reducing non-radiative recombination.[58,59]

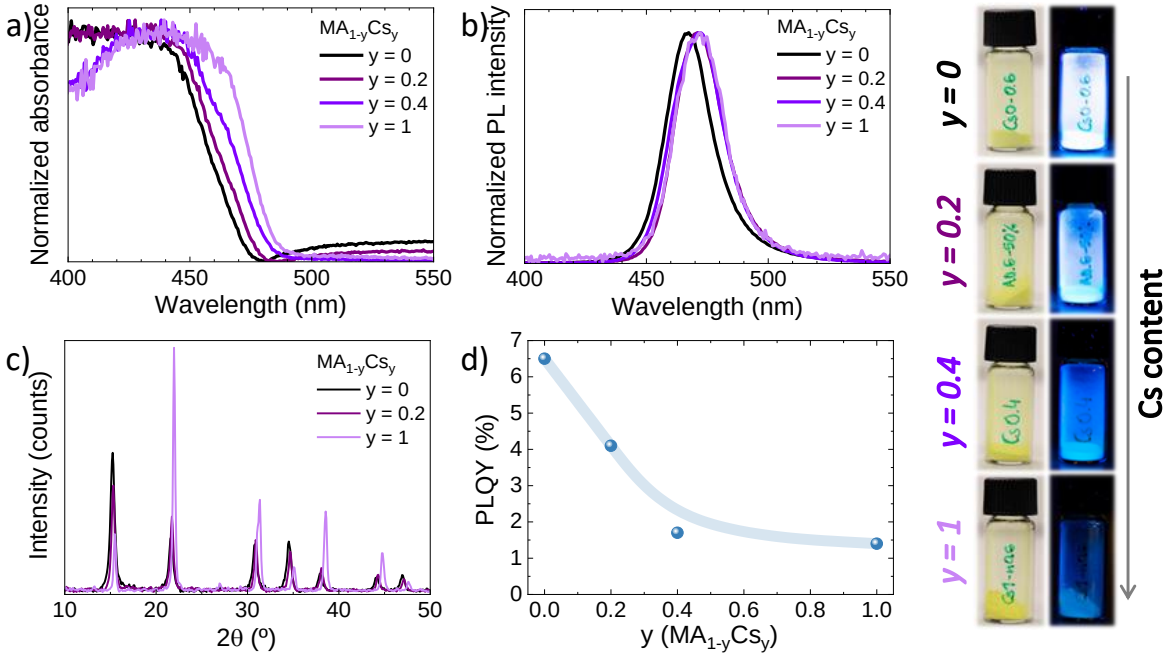

Figure 3. a) Absorption and b) photoluminescence spectra for the mechanochemically synthesized $MA_{1-y}Cs_yPb(Br_{0.6}Cl_{0.4})_3$ samples, with y = 0, 0.2, 0.4 and 1. c) XRD patterns for the same compound series and d) PLQY as a function of the Cs^+ content (the line is a guide to the eye). On the right, pictures of the samples with increasing Cs/MA ratio under ambient (left) and UV (right) light.

The simple mechanochemical synthesis is ideal for the preparation of complex perovskite compositions, hence we also studied the effect of the halide exchange on the optical characteristics of the perovskite series, in particular the relationship between the bandgap and the PLQY. The synthesis was carried out modifying the content of all the different precursors, adjusting the ratio of both MABr/MACl and $PbBr_2/PbCl_2$, and keeping constant the concentration of AmCl at 50 mol%. The bromide content was increased from 0 to 1 in the preparation of 6 different perovskites of the type $MAPb(Br_nCl_{1-n})_3$. **Figure 4**a and b show the optical absorption and PL spectra, respectively, for the entire sample series.

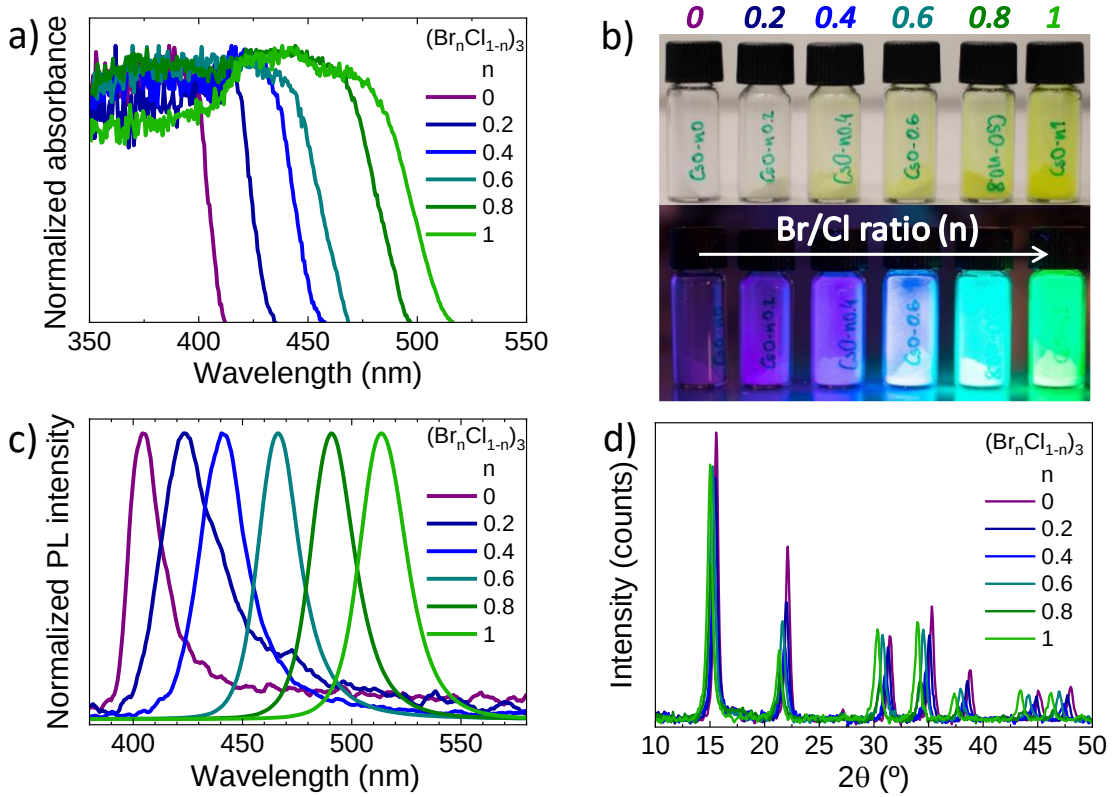

Figure 4. a) Absorbance and b) PL spectra of the $MAPb(Br_nCl_{1-n})_3$ samples for n = 0, 0.2, 0.4, 0.6, 0.8 and 1. c) Pictures of the mentioned samples with a varying Br/Cl content under ambient light (top) and UV light (λ = 365 nm) (bottom). d) XRD analysis of all the samples.

The samples exhibited absorption onsets red-shifting from 410 nm (n = 0, pure chloride compound) to 512 nm (n = 1, pure bromide perovskite) as the bromide content is increased. The corresponding PL maxima follows the same trend, decreasing in energy from 405 nm (violet) to 514 nm (green) for pure chloride and bromide materials, respectively. The CIE coordinates calculated from the PL spectra of the different samples are reported in Figure S4. XRD analysis (Figure 4d) confirmed the formation of highly crystalline pure chloride and bromide perovskites, as well as for the mixed halide species. The XRD patterns show a displacement of the signals corresponding to the same planes to smaller angles as the Br/Cl ratio increases (a more detailed comparison of the diffractogram can be found in Figure S5). As the bandgap narrows, the associated PLQY raise from approximately 1% (for $0 \leq n \leq 0.4$) to

7% (n = 0.6), and up to 15% and 29% for the bromide-rich, green-emitting $MAPb(Br_nCl_{1-n})_3$ (n = 0.8 and 1, respectively). We also performed the mechanochemical synthesis of the same series of materials, but now substituting 20% of MA^+ with Cs^+. The structural and optical characterization (Figure S6), are very similar to those presented in Figure 4, and we observed slightly lower PLQY (1% and 25% for the pure chloride and pure bromide compounds, respectively), which is consistent with the trend observed for higher caesium content materials (Figure 3). Although we cannot exclude differences in the formation chemistry of the materials, the large increase in PLQY observed when decreasing the bandgap from blue-emitting (7%) to green-emitting (29%) perovskites is likely related to the energy and distribution of trap states with respect to the electronic bands of the semiconductors. Quenching, deep traps in blue perovskites become shallower or fall within the electronic bands when the bandgap is decreased, as discussed previously.

In summary, we have prepared a series of highly luminescent lead halide perovskites powders leveraging the benefits of mechanochemical synthesis. Mechanochemical synthesis is a simple, solvent-free method, useful to prepare perovskites with virtually any composition. Importantly, mechanochemical synthesis is a valuable tool to investigate complex materials and the direct effect of additives on their properties, without the limitation in terms of solubility and crystallization kinetics which are unavoidable in solution-processed perovskites. We have synthesised compounds whose emission colour can be tuned from the violet to the green, and with enhanced photoluminescence efficiency thanks to the use of the additive amantadine hydrochloride (AmCl). The addition of AmCl was optimized and a 50 mol% loading was found to lead to the highest photoluminescence quantum yield for these specific compounds and with the experimental conditions used. The use of the passivating molecule produces a decrease of the non-radiative recombination pathways without modifying the structure of the synthesised materials, leading to an increase of the PLQY from 0 to 5% in the blue, and up to 29% for green-emitting bulk powders.

Experimental Section

Mechanochemical synthesis: $MA_{0.8}Cs_{0.2}Pb(Br_{0.6}Cl_{0.4})_3$ was prepared by ball-milling; 0.48 mol of CH_3NH_3Br (MABr), 0.32 mol of CH_3NH_3Cl (MACl), 0.12 mol of CsBr and 0.08 mol of CsCl were mixed together with 0.6 mol of $PbBr_2$ and 0.4 mol of $PbCl_2$ inside a nitrogen-filled glovebox. The powder mixture was then introduced in a 10 mL zirconia ball-mill jar with zirconia beads. Afterwards, ball-milling was performed at a frequency of 30 Hz for 2 hours. The resulting yellowish powder was then studied as obtained in ambient conditions and at room temperature. The passivated samples were obtained adding an increasing amount (from 0 to 90 mol%) of amantadine hydrochloride (AmCl) to the mixture before ball-milling. For the rest of the $MA_yCs_{1-y}Pb(Br_nCl_{1-n})_3$ samples, MAX/CsX and Br^-/Cl^- were adjusted accordingly. Cs molar ratio was varied from 0 (pure $MAPb(Br_nCl_{1-n})_3$) to 1 (pure $CsPb(Br_nCl_{1-n})_3$). Br molar ratio was varied from 0 (pure $MA_yCs_{1-y}PbCl_3$) to 1 (pure $MA_yCs_{1-y}PbBr_3$). See Tables S1, S2 and S3 for the precursors quantities of the different samples.

Characterization: The photoluminescence (PL) spectra were taken using a 375 nm laser excitation source and a spectrometer (Hamamatsu C9920-02 with a Hamamatsu PMA-11 optical detector). PLQY values were obtained using a Xe lamp coupled to a monochromator as the excitation source and an integrated sphere coupled to a spectrometer (Hamamatsu C9920-02 with a Hamamatsu PMA-11 optical detector). The instrumental error is approximately 1%. UV-visible absorption spectra of the films were collected in an integrated sphere using a fiber-optics based Avantes Avaspec2048 spectrophotometer. X-ray diffraction was measured with a Panalytical Empyrean diffractometer equipped with CuKα anode operated at 45 kV and 30 mA and a Pixel 1D detector in scanning line mode. Single scans were acquired in the 2 theta = 5° to 50° range in Bragg-Brentano geometry in air. Data analysis was performed with HighScore Plus software.

Supporting Information

Supporting Information is available from the Wiley Online Library or from the author.

Acknowledgments

The research leading to these results has received funding from the European Union Programme for Research and Innovation Horizon 2020 (2014–2020) under the Marie Skłodowska-Curie Grant Agreement PerovSAMs No. 747599 and the Spanish Ministry of Economy and Competitiveness (MINECO) via the Unidad de Excelencia María de Maeztu MDM-2015-0538, MAT2017-88821-R, PCIN-2015-255, PCIN-2017-014, and the Generalitat Valenciana (Prometeo/2016/135). M.S. acknowledges the MINECO for his RyC contracts.

Received: ((will be filled in by the editorial staff))
Revised: ((will be filled in by the editorial staff))
Published online: ((will be filled in by the editorial staff))

References

[1] L. N. Quan, B. P. Rand, R. H. Friend, S. G. Mhaisalkar, T.-W. Lee, E. H. Sargent, *Chem. Rev.* **2019**, *119*, 7444.
[2] A. K. Jena, A. Kulkarni, T. Miyasaka, *Chem. Rev.* **2019**, *119*, 3036.
[3] T. Leijtens, K. A. Bush, R. Prasanna, M. D. McGehee, *Nat. Energy* **2018**, *3*, 828.
[4] F. P. García de Arquer, A. Armin, P. Meredith, E. H. Sargent, *Nat. Rev. Mater.* **2017**, *2*, 16100.
[5] H. Wei, J. Huang, *Nat. Commun.* **2019**, *10*, 1066.
[6] Gurudayal, J. Ager, N. Mathews, in *Halide Perovskites*, Wiley-VCH Verlag GmbH & Co. KGaA, Weinheim, Germany, **2018**, pp. 273–292.
[7] X. Zhao, H. Xu, Z. Wang, Y. Lin, Y. Liu, *InfoMat* **2019**, *1*, inf2.12012.
[8] R. A. John, N. Yantara, Y. F. Ng, G. Narasimman, E. Mosconi, D. Meggiolaro, M. R. Kulkarni, P. K. Gopalakrishnan, C. A. Nguyen, F. De Angelis, S. G. Mhaisalkar, A. Basu, N. Mathews, *Adv. Mater.* **2018**, *30*, 1805454.
[9] W. Li, Z. Wang, F. Deschler, S. Gao, R. H. Friend, A. K. Cheetham, *Nat. Rev. Mater.* **2017**, *2*, 16099.
[10] J. Huang, Y. Yuan, Y. Shao, Y. Yan, *Nat. Rev. Mater.* **2017**, *2*, 17042.
[11] J. M. Ball, A. Petrozza, *Nat. Energy* **2016**, *1*, 16149.
[12] B. R. Sutherland, E. H. Sargent, *Nat. Photonics* **2016**, *10*, 295.
[13] T. M. Brenner, D. A. Egger, L. Kronik, G. Hodes, D. Cahen, *Nat. Rev. Mater.* **2016**, *1*,

15007.
[14] R. Swartwout, M. T. Hoerantner, V. Bulović, *Energy Environ. Mater.* **2019**, *2*, 119.
[15] Z. Li, T. R. Klein, D. H. Kim, M. Yang, J. J. Berry, M. F. A. M. van Hest, K. Zhu, *Nat. Rev. Mater.* **2018**, *3*, 18017.
[16] W. Zhang, M. Saliba, D. T. Moore, S. K. Pathak, M. T. Hörantner, T. Stergiopoulos, S. D. Stranks, G. E. Eperon, J. A. Alexander-Webber, A. Abate, A. Sadhanala, S. Yao, Y. Chen, R. H. Friend, L. A. Estroff, U. Wiesner, H. J. Snaith, *Nat. Commun.* **2015**, *6*, 6142.
[17] N. K. Noel, S. N. Habisreutinger, B. Wenger, M. T. Klug, M. T. Hörantner, M. B. Johnston, R. J. Nicholas, D. T. Moore, H. J. Snaith, *Energy Environ. Sci.* **2017**, *10*, 145.
[18] H. Zhang, M. K. Nazeeruddin, W. C. H. Choy, *Adv. Mater.* **2019**, *31*, 1805702.
[19] P. Wang, Y. Wu, B. Cai, Q. Ma, X. Zheng, W.-H. Zhang, *Adv. Funct. Mater.* **2019**, *0*, 1807661.
[20] M. Jung, S.-G. Ji, G. Kim, S. Il Seok, *Chem. Soc. Rev.* **2019**, *48*, 2011.
[21] Y. Zhang, S. G. Kim, D. K. Lee, N. G. Park, *ChemSusChem* **2018**, *11*, 1813.
[22] D. Prochowicz, P. Yadav, M. Saliba, M. Saski, S. M. Zakeeruddin, J. Lewiński, M. Grätzel, *ACS Appl. Mater. Interfaces* **2017**, *9*, 28418.
[23] Y. El Ajjouri, F. Palazon, M. Sessolo, H. J. Bolink, *Chem. Mater.* **2018**, *30*, 7423.
[24] L. Protesescu, S. Yakunin, O. Nazarenko, D. N. Dirin, M. V. Kovalenko, *ACS Appl. Nano Mater.* **2018**, *1*, 1300.
[25] P. Sadhukhan, S. Kundu, A. Roy, A. Ray, P. Maji, H. Dutta, S. K. Pradhan, S. Das, *Cryst. Growth Des.* **2018**, *18*, 3428.
[26] Z. Hong, D. Tan, R. A. John, Y. K. E. Tay, Y. K. T. Ho, X. Zhao, T. C. Sum, N. Mathews, F. García, H. Sen Soo, *iScience* **2019**, *16*, 312.
[27] S. Yun, A. Kirakosyan, S. G. Yoon, J. Choi, *ACS Sustain. Chem. Eng.* **2018**, *6*, 3733.
[28] F. Palazon, Y. El Ajjouri, H. J. Bolink, *Adv. Energy Mater.* **2019**, *1902499*, 1.
[29] J.-J. Nath, Narayan Chandra Deb; Murugadoss, Gavindasamy; Lee, *Nanosci. Nanotechnol. Lett.* **2018**, *10*, 1025.
[30] N. Leupold, K. Schötz, S. Cacovich, I. Bauer, M. Schultz, M. Daubinger, L. Kaiser, A. Rebai, J. Rousset, A. Köhler, P. Schulz, R. Moos, F. Panzer, *ACS Appl. Mater. Interfaces* **2019**, *11*, 30259.
[31] P. Fan, D. Gu, G. X. Liang, J. T. Luo, J. L. Chen, Z. H. Zheng, D. P. Zhang, *Sci. Rep.* **2016**, *6*, 1.
[32] G. Longo, L. Gil-Escrig, M. J. Degen, M. Sessolo, H. J. Bolink, *Chem. Commun.* **2015**, *51*, 7376.
[33] J. Ávila, C. Momblona, P. P. Boix, M. Sessolo, H. J. Bolink, *Joule* **2017**, *1*, 431.
[34] M. J. Crane, D. M. Kroupa, J. Y. Roh, R. T. Anderson, M. D. Smith, D. R. Gamelin, *ACS Appl. Energy Mater.* **2019**, *2*, 4560.
[35] F. Panzer, D. Hanft, T. P. Gujar, F. J. Kahle, M. Thelakkat, A. Köhler, R. Moos, *Materials (Basel).* **2016**, *9*, DOI: 10.3390/ma9040277.
[36] J. H. Noh, S. H. Im, J. H. Heo, T. N. Mandal, S. Il Seok, *Nano Lett.* **2013**, *13*, 1764.
[37] I. Levchuk, A. Osvet, X. Tang, M. Brandl, J. D. Perea, F. Hoegl, G. J. Matt, R. Hock, M. Batentschuk, C. J. Brabec, *Nano Lett.* **2017**, *17*, 2765.
[38] Q. A. Akkerman, V. D'Innocenzo, S. Accornero, A. Scarpellini, A. Petrozza, M. Prato, L. Manna, *J. Am. Chem. Soc.* **2015**, *137*, 10276.
[39] A. Sadhanala, S. Ahmad, B. Zhao, N. Giesbrecht, P. M. Pearce, F. Deschler, R. L. Z. Hoye, K. C. Gödel, T. Bein, P. Docampo, S. E. Dutton, M. F. L. De Volder, R. H. Friend, *Nano Lett.* **2015**, *15*, 6095.
[40] J. Xing, Y. Zhao, M. Askerka, L. N. Quan, X. Gong, W. Zhao, J. Zhao, H. Tan, G. Long, L. Gao, Z. Yang, O. Voznyy, J. Tang, Z.-H. Lu, Q. Xiong, E. H. Sargent, *Nat.*

Commun. **2018**, *9*, 3541.
[41] Y. Liu, J. Cui, K. Du, H. Tian, Z. He, Q. Zhou, Z. Yang, Y. Deng, D. Chen, X. Zuo, Y. Ren, L. Wang, H. Zhu, B. Zhao, D. Di, J. Wang, R. H. Friend, Y. Jin, *Nat. Photonics* **2019**, DOI: 10.1038/s41566-019-0505-4.
[42] S. D. Stranks, V. M. Burlakov, T. Leijtens, J. M. Ball, A. Goriely, H. J. Snaith, *Phys. Rev. Appl.* **2014**, *2*, 1.
[43] M. C. Brennan, S. Draguta, P. V. Kamat, M. Kuno, *ACS Energy Lett.* **2018**, *3*, 204.
[44] S. J. Yoon, S. Draguta, J. S. Manser, O. Sharia, W. F. Schneider, M. Kuno, P. V. Kamat, *ACS Energy Lett.* **2016**, *1*, 290.
[45] N. K. Noel, A. Abate, S. D. Stranks, E. S. Parrott, V. M. Burlakov, A. Goriely, H. J. Snaith, *ACS Nano* **2014**, *8*, 9815.
[46] D. S. Lee, J. S. Yun, J. Kim, A. M. Soufiani, S. Chen, Y. Cho, X. Deng, J. Seidel, S. Lim, S. Huang, A. W. Y. Ho-Baillie, *ACS Energy Lett.* **2018**, *3*, 647.
[47] X. Li, C. C. Chen, M. Cai, X. Hua, F. Xie, X. Liu, J. Hua, Y. T. Long, H. Tian, L. Han, *Adv. Energy Mater.* **2018**, *8*, 1.
[48] J. Idígoras, F. J. Aparicio, L. Contreras-Bernal, S. Ramos-Terrón, M. Alcaire, J. R. Sánchez-Valencia, A. Borras, Á. Barranco, J. A. Anta, *ACS Appl. Mater. Interfaces* **2018**, *10*, 11587.
[49] D. M. Jang, K. Park, D. H. Kim, J. Park, F. Shojaei, H. S. Kang, J. P. Ahn, J. W. Lee, J. K. Song, *Nano Lett.* **2015**, *15*, 5191.
[50] N. K. Kumawat, X.-K. Liu, D. Kabra, F. Gao, *Nanoscale* **2019**, *11*, 2109.
[51] P. Audebert, G. Clavier, V. Alain-Rizzo, E. Deleporte, S. Zhang, J.-S. Lauret, G. Lanty, C. Boissière, *Chem. Mater.* **2009**, *21*, 210.
[52] W. Yi, *Thesis* **2012**, 1.
[53] Q.-L. Li, W.-X. Lu, N. Wan, S.-N. Ding, *Chem. Commun.* **2016**, *52*, 12342.
[54] M. M. Tavakoli, W. Tress, J. V Milić, D. Kubicki, L. Emsley, M. Grätzel, *Energy Environ. Sci.* **2018**, *11*, 3310.
[55] Y. Cui, J. Ren, G. Chen, W. Yu, Y. Qian, *Acta Crystallogr. Sect. C Cryst. Struct. Commun.* **2000**, *56*, e552.
[56] E. T. Hoke, D. J. Slotcavage, E. R. Dohner, A. R. Bowring, H. I. Karunadasa, M. D. McGehee, *Chem. Sci.* **2015**, *6*, 613.
[57] M. R. Linaburg, E. T. McClure, J. D. Majher, P. M. Woodward, *Chem. Mater.* **2017**, *29*, 3507.
[58] G. Nan, X. Zhang, M. Abdi-Jalebi, Z. Andaji-Garmaroudi, S. D. Stranks, G. Lu, D. Beljonne, *Adv. Energy Mater.* **2018**, *8*, 1702754.
[59] H. Tan, F. Che, M. Wei, Y. Zhao, M. I. Saidaminov, P. Todorović, D. Broberg, G. Walters, F. Tan, T. Zhuang, B. Sun, Z. Liang, H. Yuan, E. Fron, J. Kim, Z. Yang, O. Voznyy, M. Asta, E. H. Sargent, *Nat. Commun.* **2018**, *9*, DOI: 10.1038/s41467-018-05531-8.

Bright photoluminescent wide bandgap mixed-halide 3D perovskites are prepared by dry mechanochemical synthesis starting from neat binary precursors, and show enhanced photoluminescence upon the addition of an adamantane derivative in the precursors mixture. Photoluminescence quantum yields as high as 29% and 5% has been obtained for green- and blue-emitting perovskite solids.

Keyword perovskite, mechanochemical synthesis, photoluminescence, blue, passivation

L. Martínez-Sarti, F. Palazon, M. Sessolo* and H. J. Bolink

Dry mechanochemical synthesis of highly luminescent, blue and green hybrid perovskite solids

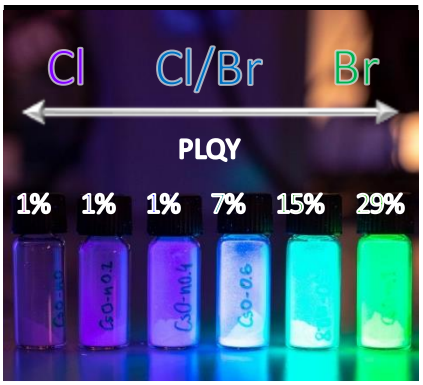
Cl
Cl/Br
Br
PLQY
1%
1%
1%
7%
15%
29%